Pergamon

Cement and Concrete Research 31 (2001) 555–561

CEMENT AND CONCRETE RESEARCH

Determination by nanoindentation of elastic modulus and hardness of pure constituents of Portland cement clinker

Karine Velez[a], Sandrine Maximilien[a], Denis Damidot[b], Gilbert Fantozzi[a], Fransois Sorrentino[b,*]

[a]*INSA, GEMPPM, 20 Avenue Albert Einstein, 69621 Villeurbanne, France*
[b]*Lafarge Central Laboratory, 95 rue du Montmurier, BO 15, 38291 Saint Quentin Fallavier, France*

Received 24 January 2000; accepted 8 December 2000

Abstract

The mechanical properties, particularly the elastic modulus and the hardness of the major phases of Portland cements (C_3S and alite, C_2S and belite, C_3A, C_4AF) are measured at the microscopic scale by nanoindentation and at the macroscopic scale by the resonance frequencies technique. At the microscopic scale, the elastic moduli of these phases range between 125 and 145 GPa. The hardness of the calcium aluminate (C_3A) is around 10 GPa while those of the silicates are lower (8 to 9 GPa). There are no significant differences between the elastic properties of the pure phases (C_3S, C_2S) and those of their solid solution alite and belite found in industrial clinker. The results found at the macroscopic scale takes into account the bulk porosity of the samples. The elastic moduli of the C_3S, C_2S, C_3A phases decrease by about 35% when the porosity decreases by 15%. The elastic moduli obtained at the macroscopic scale, by extrapolation at zero porosity, are in good agreement with the results obtained at the microscopic scale by nanoindentation.

Keywords: Mechanical properties; Elastic moduli; Micromechanics; Clinker

1. Introduction

The improvement achieved during the last decade from the ordinary concrete to the high-performance concrete (HPC), very-high-performance concrete (VHPC) and to the reactive powder concrete (RPC) is mainly due to a better understanding of the microstructure of the material [1]. The microstructure of the hardened concrete depends on the design of the concrete (proportion, quality of the starting material, ...), processing, curing, and on the rate of the hydration of the cement [2]. The knowledge of the properties of the different constituents involved in the final microstructure is consequently essential to improve the concrete. There are calcium silicate hydrates, residual clinker, aggregates, fibers, ...

Modelling the microstructure is a promising way to highlight the important parameters and reduce the quantity of tests. It requires determining mechanical properties of the residual clinker, hydrated phases and aggregates or other additions such as fibers. This paper deals with the elastic modulus and the hardness of the principal minerals contained in Portland cement. A second study, published further, is devoted to the measurement of the elastic properties of calcium silicate hydrates.

Modelling is very often limited by the lack of data concerning the mechanical features of the materials (elastic modulus, hardness) and more specifically, by the lack of data obtained in situ (locally in the concrete matrix). Very little information is found in the literature [3,4].

In the present paper, the measurements are carried out at the microscopic scale by nanoindentation in order to obtain local measurements, and at the macroscopic scale by resonance frequency measurements, in order to relate both scale of measurements independently on the porosity of the sample involved at the macroscopic scale.

2. Methods

2.1. Sample preparation

Pure phases related to the constituents found in Portland cement [tricalcium silicate (C_3S), dicalcium silicate (C_2S),

* Corresponding author. Tel.: +33-4-7682-1771; fax: +33-4-7495-5623.
E-mail address: francois.sorrentino@pole-technologique.lafarge.com (F. Sorrentino).

0008-8846/00/$ – see front matter
PII: S0008-8846(00)00505-6

tricalcium aluminate (C_3A), calcium aluminoferrite (C_4AF)] have been synthesized from reagent grade oxide and calcium carbonate. Synthetic alite and belite have also been prepared in the same way by adding Al_2O_3, Fe_2O_3, MgO in the proportion corresponding to an average industrial clinker [5]. The structure and the purity of the synthesised phases were checked by X-ray diffraction. The samples devoted to the nanoindentation tests are prepared by compacting slightly humidified powder at 40 MPa. The pellets are dried at 110°C and sintered at 1450°C for C_3S, C_2S, C_3A and 1350°C for C_4AF. Then, the pellets are embedded in a low-viscosity epoxy resin and polished by using, at first, abrasive papers of 400, 600 and 1200 grade and then diamond suspensions (6, 3, 1, and 0.25 μm). Careful attention is paid to the quality of the surface of the sample (flatness, cracks, and scratches) for the measurements of elastic moduli and hardness by nanoindentation to insure the reproducibility of the small penetration of the indenter. The chemical homogeneity is checked by SEM/EDS (after carbon coating of the polished section). Fifty analyses are carried out in the section and if the standard deviation of the chemical analysis is higher than 1%, the sample is rejected. Then the sample is repolished to remove the carbon coating (0.25 μm) and is ready for the nanoindentation tests.

The pressure and sintering techniques are used to obtain dense particles in order to obtain a polished section to check the chemical homogeneity and to minimize the standard deviation of the results of E and H. It is more difficult to carry out these experiments on powders. The volume of matter, which is concerned for the nanoindentation test, is about 5 μm^3 (the order of magnitude of the volume analysed by the electron beam in SEM). In this case, it is not necessary to have a large pellet of high bulk density but dense particles of few millimeters are recommended.

For the macroscopic tests (using resonance frequencies measurements method), prism specimens are prepared with humidified powders compacted at 40 MPa. The specimens are dried at 110°C and sintered at 1450°C for C_3S, C_2S, C_3A and 1350°C for C_4AF. In this case, the target is to obtain a large sample with a high bulk density. In order to obtain different porosity for every sample, two powders with a different specific area are mixed by varying the quantity of each powder to have an extended particle size distribution. The porosity of the samples is deduced from the comparison between the measured and the theoretical density.

2.2. Experimental procedures

The experiments at the microscopic scale by nanoindentation were performed using a Nanoindentation TM II shown schematically in Fig. 1. The instrument continuously monitors the displacement of the indenter by a capacitance gauge as a load is applied. The load and

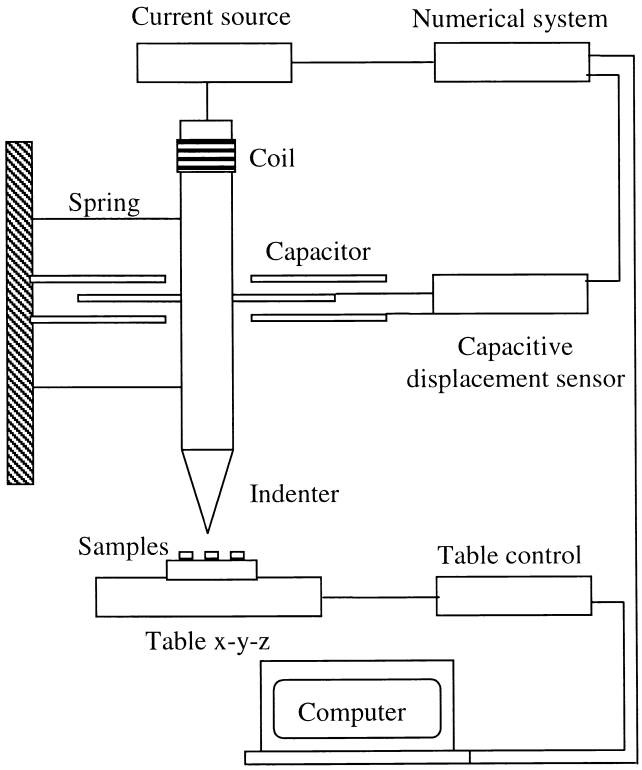

Fig. 1. A schematic representation of experimental equipment used to perform the indentation experiments.

displacements resolutions of the apparatus are respectively 75 nN and 0.04 nm. The measurements of hardness and elastic modulus were obtained using a Berkovich indenter, i.e., three-sided pyramid diamond, with the same nominal area to depth relationships as the standard Vickers pyramid.

Experiments were performed using a load–time sequence that is shown in Fig. 2. The indenter was first loaded and then unloaded three times at a constant rate of loading. In order to insure that the contact was maintained between the specimen and the indenter, the load reached at the end of unloading is 10% of the maximum load (i.e., if the maximum load is 40 mN, the minimum is 4 mN, see Fig. 2). The multiple loadings and unloadings are necessary to check the reversibility of the deformation and thereby to make sure that the unloading data used for analysis purpose are mainly elastic. Every three unloading, the load was held constant for a period of 100 s (“hold” period) at 10% of the peak value while the displacement was carefully monitored to establish the ratio of displacement produced by thermal expansion in the system.

The system is thermally buffered from its surrounding and from the room within which it is housed. The room is temperature controlled within 1°C. However, thermal fluctuations are caused by some components of the apparatus. To account for the thermal variations, the rate of displacement was measured during the “hold” period and the

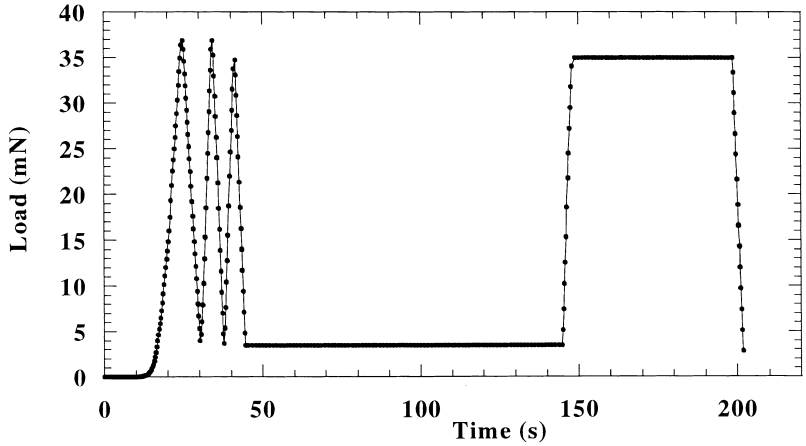

Fig. 2. Typical displacement–time sequence.

displacement data were corrected by assuming that the temperature drift rate was constant through out the entire test. Following the "hold" period, the specimen was loaded for a fourth and final time, with another 50-s "hold" period during the peak load, to avoid plastic effects, and finally, the specimen was fully unloaded.

The simultaneous measurement of the load and the displacement during the indentation allows a direct measurement of the elastic modulus and the hardness without direct imaging of the indentation using the method described by Oliver and Pharr [6,7] and developed by Boudoukha [8] for ceramics.

The relations used to computing the hardness, H, and the effective indentation modulus, E_r, from the measured data are (Eqs. (1) and (2)):

$$H = \frac{P_{max}}{A_c} \tag{1}$$

$$S = \frac{dP}{dh} = \beta \frac{2}{\sqrt{\pi}} \sqrt{A} E_r \tag{2}$$

where P_{max} is the peak load at the maximum of the curve, h is the displacement, A_c is contact area, S the contact stiffness, and β is a correction factor (approximately equal to 1.034 for the Berkovich indenter [6]). For the indentation data studied in this paper, 90% of the unloading curve was fitted to the relation described by Oliver and Pharr used to determine the contact stiffness S.

Eq. (2), which follows an analytical solution derived by Sneddon [9] for the penetration of an elastic half space by an axisymmetric indenter of arbitrary smooth profile, relates the experimental stiffness and the contact area to the effective elastic modulus.

From the measurement of the effective modulus, E_r, the elastic modulus of the material, E, is obtained using the equation (Eq. (3)):

$$\frac{1}{E_r} = \frac{1-\nu^2}{E} + \frac{1-\nu_i^2}{E_i} \tag{3}$$

where ν_i and E_i are the Poisson coefficient and the elastic properties of the diamond indenter and ν is the Poisson coefficient of the measured phase.

The experiments at the macroscopic scale were performed by the resonance frequencies technique. This type of measurement is commonly used for testing mortar and concrete [10,11]. In the resonance method, the test specimen is made to vibrate as a whole in one of its natural frequency modes (transverse, longitudinal, or torsional). The resonance frequency depends on the geometry of the sample, on its density, its pores distribution, and on the elastic properties. We use prisms in our experiments.

3. Experimental results and discussion

3.1. Nanoindentation results

The elastic modulus and the hardness of C_3S, alite, C_2S, belite, C_3A, C_4AF, are measured by nanoindentation at penetration depths of about 300 and 500 nm. Fig. 3(a–d) present the typical load–displacement curves at applied penetration of 500 nm for C_3S (a), C_2S (b), C_3A (c), and alite (d). We can notice for this penetration depth, corresponding to applied forces ranging between 40 and 50 mN, that these anhydrous phases exhibit first an elastoplastic behaviour during the first loading, and then during the successive cycles a hysteresis loop occurs. No creep phenomenom is observed at constant force. The hysteresis behaviour corresponds to an energy dissipation (damping phenomenom) probably due to a viscoelastic behaviour appearing after plastic deformation. However, this effect can be neglected in order to calculate the elastic modulus and the hardness (the elastic modulus is measured by using the last unloading curve). Table 1 shows the elastic moduli of the phases, measured at two depths of penetration. These values are an average of 10 to 20 experiments and are calculated

using an approximate Poisson's ratio of 0.3 for all constituents [7].

We check that the samples are homogeneous as the moduli and the hardness values do not vary with the penetration depth. The elastic moduli are similar to each other in the range of 125 to 145 GPa. The comparison of moduli between a pure C_3S phase and alite shows clearly that the influence of minor element included as solid solution in C_3S is not significant. The same conclusion stands for the pure C_2S and belite.

The standard deviation of the measurement is about 7%, except for C_2S and C_4AF. In the first case, this greater scatter can be explained by the polymorphic transformation during the cooling generating microcracks in the matrix. In the case of the C_4AF sample, the presence of a discontinuity was noticed on load–displacement curves (Fig. 4). This discontinuity seems to be a typical phenomenon of microcracks formation generated by the indenter during the first loadings. Such a phenomenon seems to indicate that the toughness of C_4AF phase is smaller than the one of the other anhydrous phases.

Table 2 shows the hardness of the phases, measured at two penetration depths. These values are an average of 10 to 20 experiments.

As for the elastic modulus, the hardness of the different calcium silicates are in the same range. The calcium aluminate C_3A shows a slightly stronger hardness (10.8 GPa) than silicate calcium phases (8–9 GPa.).

3.2. Resonance methods results

In order to correlate the results obtained at microscopic level to the results obtained for the bulk samples (mortar or concrete), the elastic moduli of anhydrous phases are measured at the macroscopic scale. At that scale, the values obtained integrate the intrinsic elastic modulus of the solid, but also the total porosity of the sample. To take into account the influence of the macroscopic porosity on

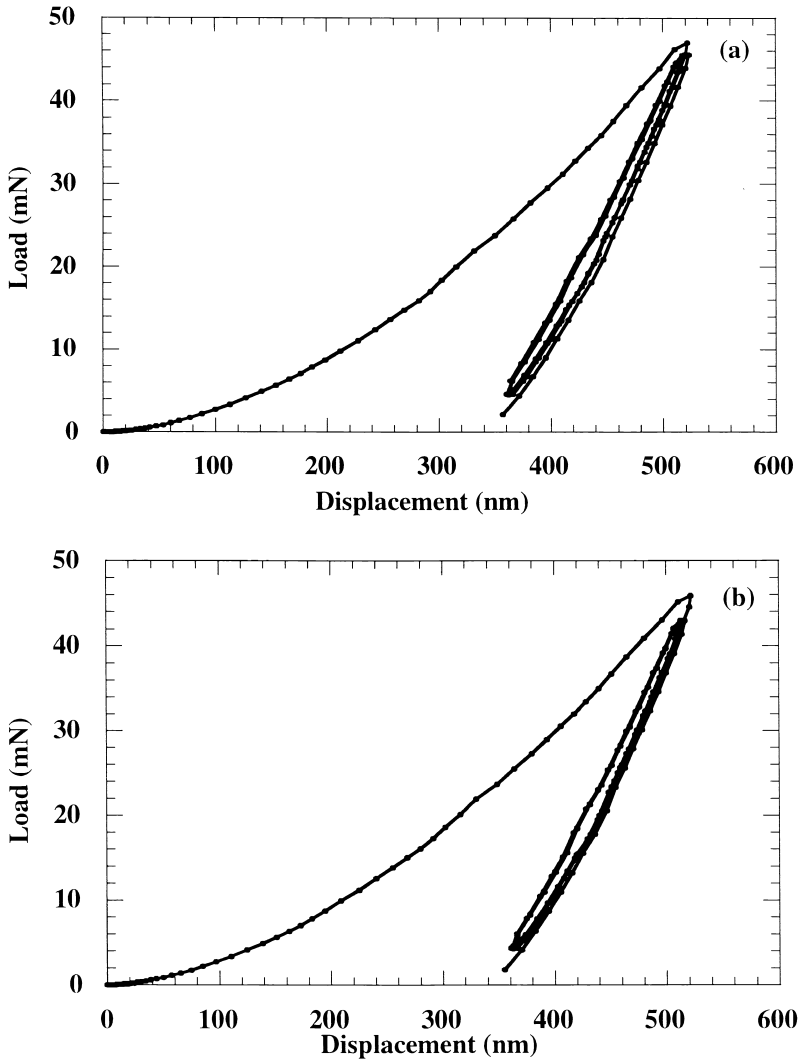

Fig. 3. Typical load–displacement curves for the anhydrous phases: (a) C_3S, (b) C_2S, (c) C_3A, (d) alite.

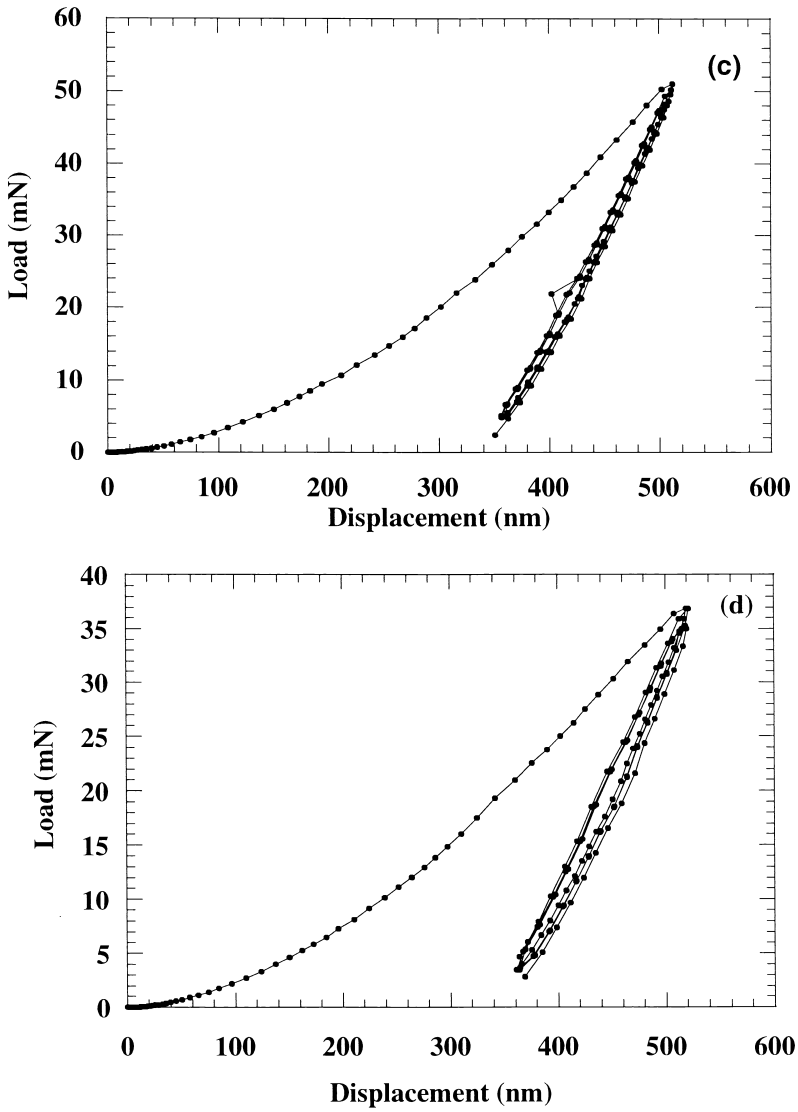

Fig. 3 (*continued*).

the elastic modulus, the dynamic moduli vs. relative porosity were determined by measuring the resonance frequency for the fundamental mode of flexural vibrations of the bar shape specimens ($10 \times 1 \times 2$ cm) [10]. For these calculations, we took, as previously, a Poisson's ratio of 0.3. By extrapolation at zero porosity, it is possible to compare these values to those obtained by the nanoindentation method.

Fig. 5(a–c), show the macroscopic dynamic moduli of C_3S, C_2S, and C_3A as a function of the relative porosity in

Table 1
Elastic moduli (E) of calcium silicates, calcium aluminate, and calcium aluminoferrite present in Portland cement clinker

	C_3S	C_2S	C_3A	C_4AF	Alite	Belite
E (GPa)	135	130	145	125	125	127
S.D.	7	20	10	25	7	10

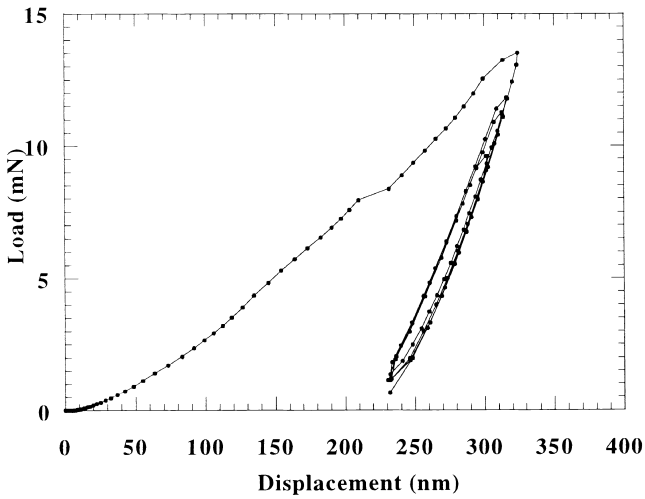

Fig. 4. Load–displacement curve for the C_4AF phase.

Table 2
Hardness (H) of calcium silicates, calcium aluminate, and calcium aluminoferrite present in Portland cement clinker

	C_3S	C_2S	C_3A	C_4AF	Alite	Belite
H (GPa)	8.7	8	10.8	9.5	9.2	8.8
S.D.	0.5	1.0	0.7	1.4	0.5	1.0

the range from 5% to 30%. We confirm that the elastic moduli decrease as the porosity increases and their evolution follows the classical polynomial relation described by Powers [12]. From 10% to 20% of porosity, the moduli decrease to about 30% to 40% depending on the samples.

Table 3
Comparison between the elastic moduli (E) obtained by nanoindentation and by resonance frequency technique for C_3S, C_2S, and C_3A

Phases	E measured by resonance frequency (GPa)/S.D.	E measured by nanoindentation/S.D.
C_3S	147/5	135/7
C_2S	140/10	130/20
C_3A	160/10	145/10

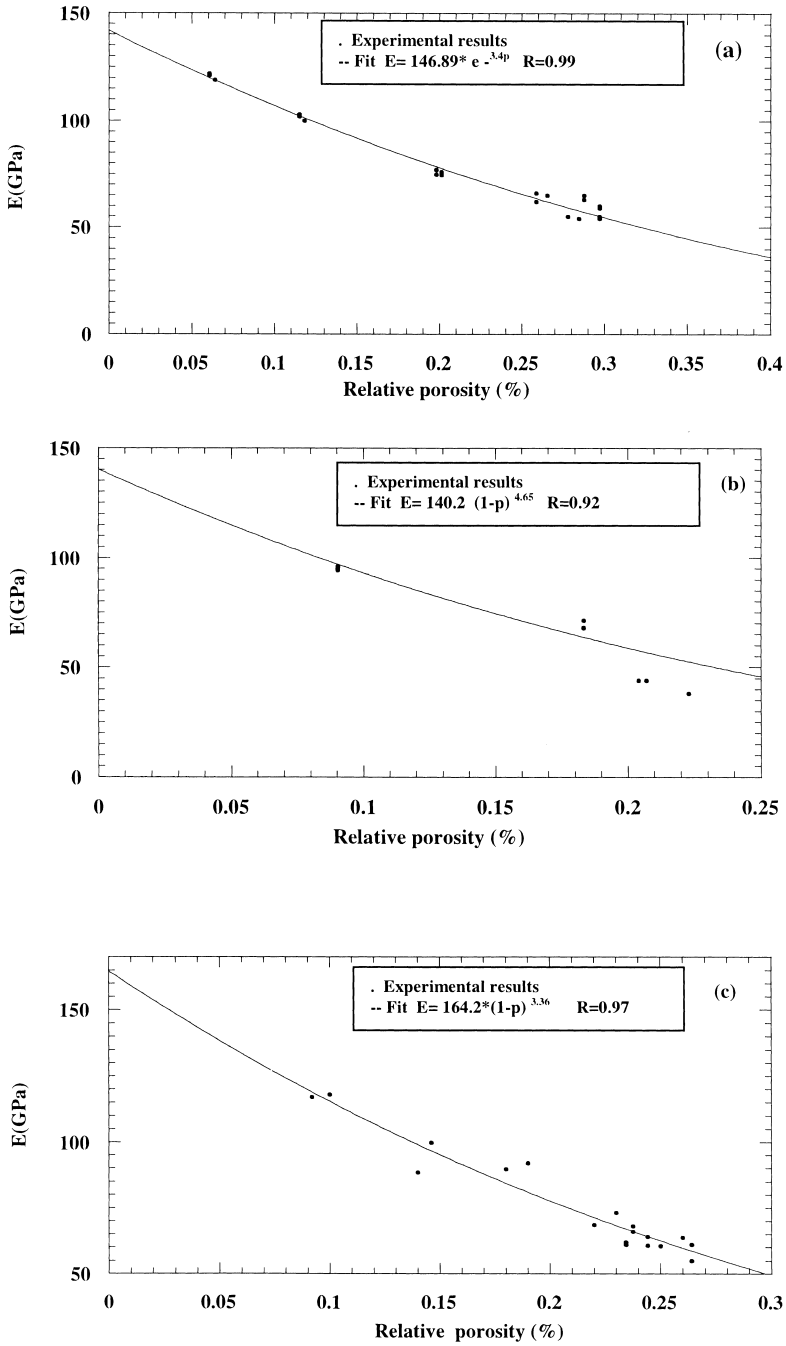

Fig. 5. Elastic moduli as a function of the relative porosity of the phases of: (a) C_3S, fit: $E = 146.89 * e^{-3.4p}$, $R = 0.99$; (b) C_2S, fit: $E = 140.2*(1-p)^{4.65}$, $R = 0.92$; (c) C_3A, fit: $164.2*(1-p)^{3.36}$, $R = 0.97$.

In the present case, the moduli obtained by extrapolation to zero porosity depend very little on the type of relation used to fit the experimental results. The values obtained using the relation $E = E_0(1-p)^n$ [12], where E_0 and p are the modulus at zero porosity, can be compared to those measured by nanoindentation (Table 3).

4. Discussion

The results obtained at the microscopic scale come from the measurement of the elastic properties of small particles (few μm^3). At this scale and being given the method of the preparation of the sample, it is easy to check that the porosity of the particles can be taken at zero (the density of the particle is close to the theoretical mass density of the compound). If the porosity were different from particles to particles, the standard deviation of the measurement would be very high. For the measurements obtained by the resonance frequency technique where the particles are agglomerated to form a prism, the porosity is due to the pores between the particles and not to the porosity of the particles themselves.

There is a good consistency between the values obtained at the macroscopic scale and those measured at the microscopic scale by nanoindentation. Very few determinations of elastic moduli of different constituents of cement are found in the literature. Granju [4] measured the elastic moduli of clinker on polished blocks. By extrapolating at zero porosity, he found an elastic modulus for the clinker ranging between 60 and 300 GPa. The scatter of the results was due to the cracks introduced during the preparation of the sample. Boumiz [3] measured the elastic modulus of compacted powder of C_3S. He prepared cylindrical samples with a density of the same order as the density of C_3S grains (3.14 g/cm^2). Assuming that the material has a zero porosity, the author found by acoustic method the elastic modulus of C_3S equal to 117 GPa. This last value is consistent with the values obtained in the present work by nanoindentation and by extrapolation method at zero porosity level.

5. Conclusions

The results found at the microscopic scale by nanoindentation showed that:

- The elastic moduli of C_3S, C_2S, C_3A, C_4AF, are similar and range between 125 and 145 GPa.
- The hardness of calcium silicate (C_3S, C_2S) and calcium aluminoferrite (C_4AF) are similar (between 8 and 9.5 GPa) and lower than the hardness of C_3A (10.8 GPa).
- There is no significant difference between the elastic moduli and the hardness of pure C_3S and the alite or between pure C_2S and belite, showing the little influence of the minor elements.

The results obtained at the macroscopic scale by frequency resonance technique showed that:

- The elastic moduli of C_3S, C_2S, C_3A, decrease as the porosity increases. From 10% to 20% of porosity, the moduli decrease from about 30% to 40%.
- The elastic moduli obtained by extrapolation at zero porosity are in good agreement with the results obtained at the microscopic scale by nanoindentation.

This work is the initial step toward developing a constitutive relationship for mechanical properties of hydrated cements. The consistency of the results obtained at the microscopic and macroscopic scales supports the use of the technique of nanoindentation to the hydrated paste of cement that is the next step of our work.

References

[1] P. Richard, M. Cheyrezy, Composition of reactive powder concretes, Cem. Concr. Res. 25 (1992) 1501–1511.
[2] M. Cheyrezy, V. Maret, L. Frouin, Microstructural analysis of RPC (reactive powder concrete), Cem. Concr. Res. 25 (1995) 1491–1500.
[3] A. Boumiz, Etude comparée des évolutions chimiques et mécaniques des pâtes de ciment et mortiers à très jeune âge, PhD thesis, Université Denis Diderot, Paris 7, France, 1995.
[4] J.L. Granju, Modélisation des pates de ciments durcies: Caractérisation de l'état d'hydratation, lois d'évolution de la résistance en compression et du module de déformation longitudinale, PhD thesis, Université Paul Sabatier de Toulouse, France, 1987.
[5] H.F.W. Taylor, Cement Chemistry, Thomas Telford, London 1997, p. 8.
[6] W.C. Oliver, G.M. Pharr, An improved technique for determining hardness and elastic modulus using load and displacement sensing indentation experiments, J. Mater. Res. 7 (1992) 1564–1583.
[7] W.C. Oliver, G.M. Pharr, On the generality of the relationship among contact stiffness, contact area and elastic modulus during indentation, J. Mater. Res. 7 (1992) 613–617.
[8] L. Boudoukha, Etude par nanoindentation de l'effet de l'implantation ionique sur le comportement mécanique de céramiques, Thèse de doctorat, INSA-Lyon 1, 1996.
[9] I.N. Sneddon, The relation between load and penetration in the axisymmetric Boussinesq problem for a punch of arbitrary profile, Int. J. Eng. Sci. 3 (1967) 47–57.
[10] S. Spinner, W.E. Tefft, A method for determining mechanical resonance frequencies and for calculating elastic moduli from these frequencies, 64th Annual Meeting of the ASTM vol. 61, (1961) 25–30 (June).
[11] L. Brunarsky, Recommendations for the use of resonance methods for testing concretes, Mater. Struct. 2 (10) (1969), 269–273.
[12] T.C. Powers, Properties of cement Portland concrete, Proceedings of the Fourth International Symposium on the Chemistry of Cement, Washington, DC vol. 2, (1960) 571–609, N.B.S., Washington.